Tellus (2007), 59A, 30–49
Printed in Singapore. All rights reserved

TELLUS

Climate variability in Scandinavia for the past millennium simulated by an atmosphere-ocean general circulation model

By ISABELLE GOUIRAND[1], ANDERS MOBERG[1,2]* and EDUARDO ZORITA[3], [1]*Department of Physical Geography and Quaternary Geology, Stockholm University, SE-106 91 Stockholm, Sweden;* [2]*Department of Meteorology, Stockholm University, SE-106 91 Stockholm, Sweden;* [3]*GKSS Research Centre, Geesthacht, Germany*

(Manuscript received 15 September 2005; in final form 28 August 2006)

ABSTRACT

The atmosphere-ocean model ECHO-G, run with solar, volcanic and greenhouse gas forcing for the past millennium, is used to analyse winter and summer temperature variability in Scandinavia. Relationships with atmospheric circulation, North Atlantic SSTs and Northern Hemisphere (NH) temperatures are investigated at timescales longer and shorter than 10 yr. The simulated response to volcanic forcing is also analysed. Realistic relationships with the atmospheric circulation, with some deficiencies in summer, are found. High-frequency co-variations with SSTs and NH temperatures are too weak, but low-frequency co-variations with NH temperatures in winter are apparently too strong. The summer cooling response to volcanic forcing is realistic, but the expected winter warming is absent. The simulated long-term temperature evolution agrees broadly with proxy data. Combinations of several forcing factors can lead to decadal and multidecadal anomalies from the centennial trends. Decreased solar forcing can account for cold intervals in both summer and winter. A systematic negative North Atlantic Oscillation (NAO) phase can explain the coldest winter temperatures during 1590–1650. Several strong volcanic forcing events can have contributed to a simultaneous summer cooling. Proxy data also indicate cold summers and winters, and a negative NAO in winter, in the same period.

1. Introduction

Inspired by early studies, for example Walker and Bliss (1932) and Bjerknes (1962), several later studies have documented strong links between atmospheric circulation and sea surface temperatures (SSTs) in the Atlantic sector and near-surface temperatures in western and northern Europe. One prominent example is the quasi-regular oscillation with slightly enhanced power at 8–10 yr timescales associated with the North Atlantic Oscillation (NAO), manifested by alternating deepening and strengthening of the Icelandic Low and opposite changes of the Azores High pressure system (Hurrell, 1995; Hurrell et al., 2003). These variations imply alternating strengthening and weakening of the westerly flow towards northern Europe, leading to variations between warmer and colder winter temperatures there. Oceanic processes in the North Atlantic Ocean, and feedbacks between the atmosphere and the ocean (Grötzner et al., 1998; Timmermann et al., 1998; Visbeck et al., 2003), can lead to regional modes with slower variations in the atmospheric circulation and thereby lead to low-frequency variations of climate in northern Europe. Large-scale modes of variability and recurrent climate regimes have been documented for different timescales, particularly in winter (Raible et al., 2001, 2005; Casty et al., 2005a, b).

Climate models, often analysed in parallel with climate reconstructions from proxy data, have proven to be successful in the above mentioned studies. On the proxy data side, reconstructions of 500 hPa sea level pressures (SLPs) over the North Atlantic/European sector (Luterbacher et al., 2002a) and the NAO index (Luterbacher et al., 2002b) 500 yr back have provided invaluable information of the past behaviour of the atmospheric circulation. Together with 500-yr long gridded temperature (Luterbacher et al., 2004; Koplaki et al., 2005) and precipitation (Pauling et al., 2006) reconstructions for Europe, there are today good possibilities to study relevant climatic processes for several centuries, as demonstrated by for example Casty et al. (2005a,b).

These various climate processes affect temperature variations in Scandinavia at different timescales. Based on analyses of long instrumental records, a number of studies have found significant relationships between variations in temperature in Scandinavia and the atmospheric circulation in winter (Chen and Hellström,

*Corresponding author.
e-mail: anders.moberg@natgeo.su.se
DOI: 10.1111/j.1600-0870.2006.00207.x

1999; Chen, 2000; Jacobeit et al., 2001; Slonosky et al., 2001), but only few studies (e.g. Moberg et al., 2003) have addressed the summer season. Relationships are rather strong in both seasons. Variability in the atmospheric circulation can account for 70% of January temperature variability in southern Scandinavia (Chen, 2000). The NAO index alone can account for more than 60% of the winter temperature variations (Jacobeit et al., 2001), but the relationship is unstable and can be rather weak in some periods (Chen and Hellström 1999; Jacobeit et al., 2001; Slonosky et al., 2001). In summer, atmospheric circulation, together with associated changes in cloud amount, can explain 65% of local temperature variations (Moberg et al., 2003).

Regional climate variations in Scandinavia are not only caused by internal variability in the circulation systems. Changes in radiative forcing caused by variations in greenhouse trace-gases, solar irradiation and volcanic aerosols can also affect the regional climate. Rather little is known in detail how these factors have affected Scandinavian climate in the past, but the relative roles of externally forced and internal climate variability on larger scales have been analysed in coupled atmosphere-ocean general circulation models (AOGCMs). Yoshimori et al. (2005) analysed these relations for the Maunder Minimum period (1645–1715), which is a period when the solar irradiance and greenhouse gas forcing is supposed to have been weaker than presently. They found that a mean cooling signal is masked by internal unforced variability in northern Europe and some other regions in the Northern Hemisphere (NH). The same authors also found a clear response pattern to volcanic eruptions, where the volcanic forcing is projected onto the positive NAO pattern. This leads to a warming in winters in Scandinavia in the first few winters after strong volcanic eruptions, in agreement with previous observational and theoretical studies (e.g. Robock, 2000). Another model study by Rind et al. (2004) shows that either the weakened solar forcing during the Maunder Minimum, or lower greenhouse gas concentrations compared to the present, can produce a negative NAO phase. This should lead to colder winter temperatures in Scandinavia. It follows that Scandinavian temperature variations can be due to many different processes, which can interact in a complex manner.

Here, we analyse temperature variations over the entire past millennium for Scandinavia, focusing on the relationships to the atmospheric circulation, SSTs and temperatures in the NH, as simulated by an AOGCM driven by reconstructed time-varying solar, volcanic and greenhouse gas forcings (González-Rouco et al., 2003; von Storch et al., 2004). This simulation has been comparatively little evaluated previously, although control simulations with the same model have been rather thoroughly analysed (e.g. Raible et al., 2001; 2005; Min et al., 2005a,b). One aim with our study is therefore to evaluate how well the forced model simulates the Scandinavian climate. In addition to temperature-circulation relationships in both summer and winter, we also evaluate the model's response to the volcanic forcing and we compare the long-term evolution of simulated Scandinavian temperatures with temperature reconstructions based on proxy data. Another aim is to investigate processes that are relevant for Scandinavian temperature variability on interannual and decadal timescales separately.

The paper is structured as follows. Details about the model and a discussion of uncertainties in the forcings and the simulation are presented in Section 2. The data analysed from the simulation, from instrumental observations and from proxy evidence are described in Section 3. The analysis methods are presented in Section 4. Results are presented and discussed in Section 5 in the following order: (i) temporal evolution of multi-decadal temperature variability; (ii) comparison with proxy data and long instrumental series; (iii) response to volcanic forcing and (iv) relationships between near-surface temperatures and atmospheric circulation, SSTs and NH temperatures. An overall discussion of causes for the simulated Scandinavian temperature variations is made in Section 6. Conclusions are drawn in Section 7.

2. The model, the forcings and the simulation

2.1. The ECHO-G model

The AOGCM used here is ECHO-G (Legutke and Voss, 1999). Its atmospheric component is ECHAM4 (Roeckner et al., 1996) and the ocean model is HOPE-G (Wolff et al., 1997). ECHAM4 is a low-order spectral model, which has been used here with a horizontal resolution of about $3.75^\circ \times 3.75^\circ$ (triangular truncation at T30) and 19 vertical levels. The ocean model has an effective horizontal resolution of $2.8^\circ \times 2.8^\circ$ (T42), with increasing meridional resolution in the tropical regions reaching 0.5° at the equator, and has 20 vertical levels. The coupled model has been run with heat and freshwater flux corrections to avoid drift. A more detailed description can be found, for example, in Min et al. (2005a).

Min et al. (2005a) evaluated the internal variability in a 1000-yr control simulation with ECHO-G and followed up with an analysis of the El Niño–Southern Oscillation (ENSO) and the NAO in the same simulation (Min et al., 2005b). Simulated atmospheric circulation patterns in two control simulations have also been analysed by Raible et al. (2001; 2005). ECHO-G shows a good skill, globally, in simulating the seasonal mean climatology and interannual variability of near-surface temperatures, precipitation and SLP. Local variability of temperature at interannual to interdecadal timescales is reproduced realistically over the NH continents. Simulated NH wintertime spatial SLP patterns, in particular the NAO pattern, and their variability agree well with observations. ECHO-G, however, shares some systematic errors with other models, for example, a too regular ENSO. A predecessor of ECHO-G, known as ECHO, has been used to study a decadal climate cycle in the the North Atlantic Ocean (Grötzner et al., 1998). This simulated decadal mode shares many features with observed data, although the time period of oscillations is

slightly longer in the model (17 yr) compared to observations (12 yr).

2.2. External forcings

The model is forced by different greenhouse gases, volcanic eruptions and solar variability. Annual global concentrations of CO_2 and CH_4 (Fig. 1a) have been derived from air bubbles trapped in polar ice cores (Etheridge et al., 1996, 1998). N_2O concentrations (not shown) were kept constant before 1860 at 276 ppb and after this date increasing exponentially up to 307 ppb at 1990 (von Storch et al., 2004). The volcanic radiative forcing (Fig. 1b) is estimated from electrical conductivity and sulphate measurements in ice cores, as described by Crowley (2000). The solar radiative forcing history (Fig. 1c) has been estimated from concentrations of ^{10}Be in ice cores and (after 1610) from historical observations of sunspots, also as described by Crowley (2000). The volcanic and solar forcings were aggregated and rescaled to an effective solar constant used to drive the model (González-Rouco et al., 2003; von Storch et al., 2004). For the solar forcing, the chosen rescaling corresponds to a change of 0.3% between the mean during 1960–1990 and the mean during 1680–1710. The radiative forcing due to volcanic eruptions estimated by Crowley (2000) was multiplied by a factor of 4 to obtain the effective changes in the solar constant. No changes in anthropogenic aerosols or land-use changes have been considered.

There are uncertainties associated with all forcings. The greenhouse gas forcings are the least uncertain. Glacial ice offers a reliable method for determining past atmospheric concentrations of trace gases, but the method is not without problems (Etheridge et al., 1996; Robertson et al., 2001). Later estimates of CO_2 changes (Siegenthaler et al. 2005), however, confirm that the CO_2 history used here is robust. Errors in the CH_4 concentrations appear to be small (Etheridge et al., 1998).

Uncertainties in the solar and volcanic forcings are substantially larger. In both cases, the transformation of the proxy information in ice involves subjective decisions (Crowley, 2000; Robertson et al., 2001). In the case of volcanic eruptions, the forcing for specific events can differ by a factor of 4 between reconstructions by different authors (Stendel et al., 2006). In reality the volcanic dust ejected into the atmosphere can absorb and reflect both long- and short-wave radiation, and thereby induce complex dynamic interactions between the stratosphere and the troposphere (Robock, 2000). This can in turn lead to regional and seasonal effects on the near-surface temperatures. The way the volcanic forcing is imposed on the model here is not fully realistic, as it is treated only as a change in the effective solar constant. Therefore, neither the regional effects of volcanic aerosols in the long-wave range of the spectrum nor other scattering processes of solar radiation are incorporated. From the Scandinavian point of view, this may affect the model's ability to simulate the temperature response after large volcanic eruptions. In particular, a number of investigations have revealed that winter temperatures in parts of the NH extratropics can experience a warming in two to three winters immediately after large tropical eruptions (Robock and Mao, 1992, 1995; Robock, 2000, 2002; Jones et al., 2003). This winter warming at the surface is hypothesized to have a dynamical reason related to meridional temperature gradients, either in the stratosphere or the troposphere or both, which influence the state of the NAO. Previous observational (Kodera, 1994; Robock, 2000) and modelling studies (Yoshimori et al., 2005; Jones et al., 2005) have found a response of the NAO towards a more positive phase during two or three winters after an eruption. The simulated Scandinavian temperature response to large 'volcanic eruptions' in the ECHO-G simulation are investigated here.

The amplitude of past variations in solar forcing is much debated (see for instance, IPCC, 2001). It has been argued that production of ^{10}Be in the atmosphere is modulated, among other factors, by variations in the solar magnetic field, which may be related to solar activity (Lean et al., 1995; Bard et al, 2000). Hence, the ^{10}Be concentration in glacial ice cores can be regarded as a proxy for solar activity. High ^{10}Be concentrations measured in ice from the Maunder Minimum period (1645–1715) have been interpreted as an indication of weak solar irradiance in this period (Bard et al., 2000). There is, however, considerable uncertainty concerning how measured ^{10}Be variations can be translated to solar radiative forcing (Bard et al., 2000; Lean et al., 2002; Foukal et al., 2004). Evidence has been found that secular changes in the solar magnetic field, and therefore in ^{10}Be production rates, can occur in the absence of long-term solar irradiance changes (Lean et al., 2002). The high amounts of ^{10}Be during the Maunder Minimum need thus not necessarily imply weak solar irradiation. The irradiance variations over the 11-yr sunspot cycles are better known, as they can be calibrated against satellite measurements since 1979. It is estimated that the 11-yr solar irradiance variations have an amplitude of about 0.08% (Lean and Rind, 2001). Foukal et al. (2004) argue that the long-term difference in solar irradiance between the Maunder Minimum and the present may not be larger. At the other extreme among opinions is an estimate that the Maunder Minimum decrease in solar irradiance was as large as 1% (Reid, 1991; see also discussion in Bard et al., 2000). The corresponding estimate by Lean et al. (1995), which is 0.24%, is sometimes used as a standard (Tett et al., 2006; Stendel et al., 2006), but recent modelling studies have tended to use slightly smaller values (e.g. 0.2% in Rind et al., 2004; Stendel et al., 2006, and 0.14% in Yoshimori et al., 2005). The choice used here, that is, 0.3%, is not exceptional (Bauer et al., 2003) but may nevertheless be too large. Clearly, the choice of scaling of the long-term solar forcing amplitude has an effect on the amplitude of simulated low-frequency temperature variations (Stendel et al., 2006).

Another issue worth pointing out is that the forcing history does not include anthropogenic aerosols or land-use changes.

Since the contribution from these factors in reality is likely a negative trend in radiative forcing during the 20th century (Taylor and Penner, 1994; Bertrand et al., 2002; Bauer et al., 2003; Bellouin et al., 2005), their absence in the reconstructed forcing history implies that the simulated 20th century temperature warming trend can be too large.

2.3. The forced simulation

Figure 1d–e shows 30-yr-smoothed summer and winter temperature variations, averaged over both Scandinavia and the NH, as simulated with ECHO-G driven by the forcings described above. This simulation was first used by González-Rouco et al. (2003) to study the relation between simulated deep soil temperatures and near-surface air temperatures. The same simulation has later been used to study variability of mid-latitude storm activity on decadal to century timescales (Fischer-Bruns et al., 2005) and recurrent winter climate regimes in 500 hPa geopotential height fields over the North Atlantic and European sector (Casty et al., 2005a). Data from this simulation has also been used to test statistical methods for temperature reconstruction from proxy data (von Storch et al., 2004, 2006; Bürger et al., 2006). A shorter, but similarly forced, simulation was used in a study of global temperatures and the NAO, with particular focus on the Maunder Minimum period (Zorita et al., 2004). The latter study showed that the simulated NAO pattern, and its fingerprint on temperature and precipitation fields, compares well with observational data. However, a shift of the centres of action of the NAO towards the European continent was noted. Later, González-Rouco et al. (2006) presented another 1000-yr-long simulation with ECHO-G using the same forcings as above. This new simulation started from colder initial conditions compared to González-Rouco et al. (2003). The impact of this difference is manifested in the near-surface temperature data. NH mean temperatures are about 0.5° colder during 1000–1200 in the new simulation, but the difference decreases until around 1550. After about this time, NH temperatures in the two simulations follow each other closely. This suggests that González-Rouco

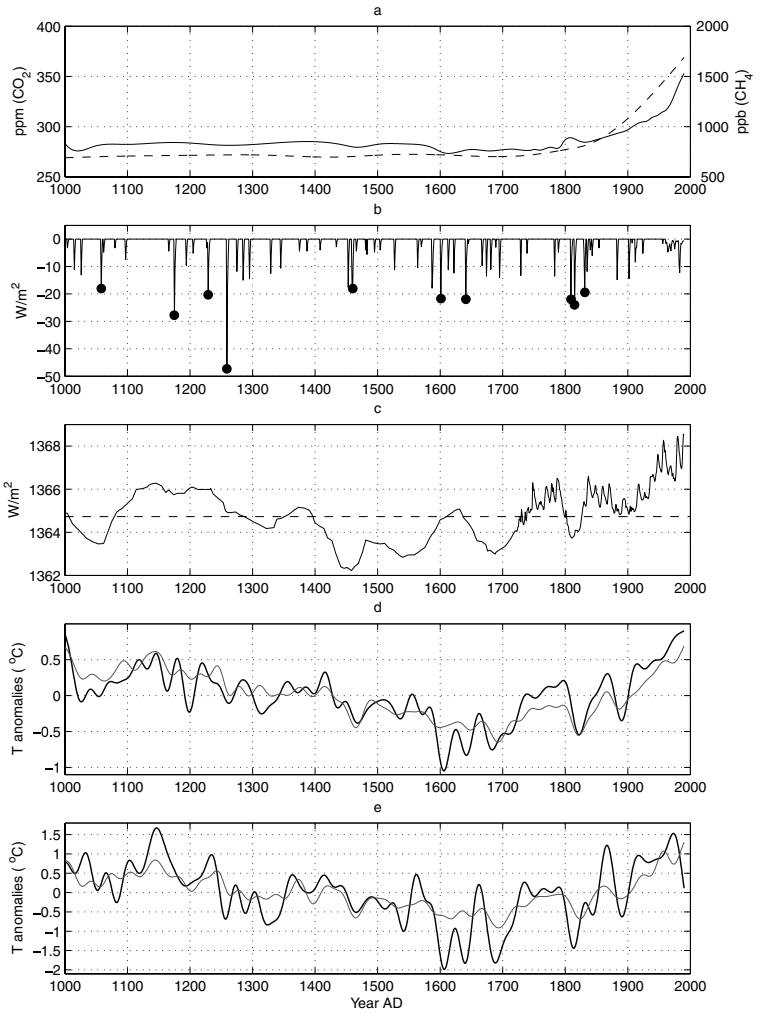

Fig. 1. Forcings and simulated temperature time-series. Atmospheric concentrations of CO_2 (solid line) and CH_4 (dashed) (a), volcanic forcing (b) and solar forcing (c). Simulated 30-yr low-pass filtered temperature anomalies 1000–1990 in Scandinavia (black) and the Northern Hemisphere (grey) in summer (JJA) (d) and winter (DJF) (e) obtained with the ECHO-G model driven by the forcings in (a–c). Temperatures are given as anomalies from the mean over the entire period. Volcanic forcing is given as its contribution to the effective solar constant. The 10 largest eruptions are denoted by black dots. The long-term mean of solar forcing is indicated with a dashed horizontal line.

et al. (2003) used a too short spin-up time, such that the model was not in equilibrium with the forcings in the early part of the simulation (Goosse et al., 2005; Osborn et al., 2006). Osborn et al. (2006) also demonstrated, by comparing ECHO-G with a simpler model, that the NH warming in the late part of the simulation is anomalously large due to the omission of anthropogenic aerosol forcing.

2.4. Can simulated Scandinavian temperatures be assessed through comparison with proxy data?

One aspect of interest is whether the temporal evolution of simulated Scandinavian near-surface temperatures over the full millennium shows a reasonably good fit with temperatures reconstructed from proxy data. A direct model versus proxy-data comparison for any specific region is, however, complicated for a number of reasons. One reason is that the true climate history represents only one possible realization out of a myriad equally possible ones given the actual forcing history (Yoshimori et al., 2005; and references therein). Similarly, a single model simulation gives just one realization among many possible temperature evolutions given the specific forcing time-series that drive the model. On a regional scale, particularly in the mid-latitudes, climate variations on interannual to decadal timescales are to a large extent due to random variations in the circulation systems. The signal-to-noise ratio for the regional temperature response to external radiative forcings is therefore rather weak. Hence, even if the reconstructed forcing history would be nearly perfect, a good fit between the time evolution of simulated and reconstructed temperatures can mainly be expected at relatively long timescales, probably longer than decadal scales. A good fit may also be expected for specific years with strong volcanic forcing—provided that the model has a realistic response. Evaluation of the long-term evolution of simulated Scandinavian temperatures is hampered also because very few proxy-based temperature reconstructions with annual resolution are available for the entire millennium, and also because they reflect only a fraction of the true climate variations only for certain parts of the year.

3. Data

We use 2 m temperatures, SSTs and SLPs for the period 1000–1990 from the simulation by González-Rouco et al. (2003). To compare the modelled data with observations, monthly $5^\circ \times 5^\circ$ gridded data sets for SLP, SST and near-surface temperatures are used. SLP data are taken from the GMSLP2 data set (Basnett and Parker, 1997). Data covering a North Atlantic and European region have been extracted. Missing values are replaced by the seasonal mean. Near-surface temperature data are taken from the HadCRUT2v data set (Jones and Moberg, 2003). SST data are taken from Kaplan Extended SST V2 (Kaplan et al., 1998). In all cases, observational data are used for the period 1874–1996.

We also use temperature data from the station with the longest instrumental record in Scandinavia. This station is Uppsala, located in southern Sweden [17.63°E; 59.87°N], which has a record that extends back to 1722. This temperature series has been homogenized to correct for changes in observation conditions, station relocations and urban warming effects (Bergström and Moberg, 2002; Moberg et al., 2003, 2005). The earliest data, however, are uncertain in winter (Bergström and Moberg, 2002). Therefore, we do not use winter data before 1750. Data after 1990 are not used because the ECHO-G simulation ends in this year.

To evaluate the temporal evolution of simulated temperatures for periods as long as possible, we employ two temperature proxy series. One is an April–August temperature reconstruction for northern Fennoscandia. The other series is a December–March temperature reconstruction for Tallinn, Estonia.

The April–August temperature reconstruction is based on tree-ring records from Northern Fennoscandia since AD 500 (Briffa et al., 1992). This reconstruction uses the regional curve standardization method to give a good estimation of the amplitude of the reconstructed long-term variations. Temperatures are estimated using regression equations, which relate variations in both density and widths of annual rings in northern Swedish Scots pines with mean temperatures for April–August in northern Fennoscandia (Briffa et al., 1992; the calibration period was 1876–1975). Here, data are used for the period 1000–1980.

The December–March temperature reconstruction (Tarand and Nordli, 2001) is a combination of instrumental temperature observations in Tallinn (with gaps filled-in using data from Stockholm and St Petersburg) for the period 1757–1997 and documentary evidence of the date of ice break-up each year in the Tallinn harbour during the period 1500–1756. The ice break-up dates have been translated to December–March temperatures using statistical relationships obtained for periods when both types of information exist (Tarand and Nordli, 2001) (these authors did not state which calibration period they used). We use data for the period 1500–1990. Unfortunately, it is not possible to evaluate the simulated winter temperatures before 1500, because no such long winter temperature reconstructions exist for the Scandinavian region.

We should mention that we also considered using a Scandinavian subset from the gridded European temperature reconstruction by Luterbacher et al. (2004), which goes 500 yr back with at least a seasonal resolution. We decided, however, not to use this reconstruction because its underlying data set contains very scarce information from Scandinavia.

4. Methods

4.1. Data pre-processing

To begin, suitable data subsets from the simulation and observations were selected and pre-processed. A Scandinavian

temperature index (Tscan) is created by averaging gridded data within the region [2.5°–27.5°E; 57.5°N–67.5°N]. This index is the primary focus in this study. We also calculate the NH mean temperatures, denoted as Tnh. SLP data are selected for the region [90°W–55°E; 20°N–70°N]. Three circulation indices, relevant for Scandinavia, are derived from these data (see Section 4.2). SST data for the North Atlantic Ocean are extracted, and and index for SSTs in the Norwegian Sea [7.5°E–7.5°W; 57.5°N–72.5°N], labelled SSTnor, is defined. The model data were interpolated to the same 5° × 5° grids as for the observations before the indices were calculated. In all cases, averages for the June–August and December–February seasons are used. For comparison with temperature proxy data, however, we use simulated April–August and December–March temperatures.

All data are subject to time-series filtering using a Butterworth filter (Raymond and Garder, 1991). For the comparison with proxy data and to study the long-term evolution of Tscan, a cut-off at 30 yr is used (Fig. 1d–e). For other analyses, the cut-off is at 10 yr. Figure 2 shows the resulting high- and low-frequency variations in Tscan, for both the model and observations. It can be seen that the amplitudes of simulated and observed Tscan are similar.

4.2. Correlation analyses

To analyse the relationship between Tscan and the atmospheric circulation patterns, SSTs and Tnh, a simple linear correlation analysis is used. Correlations are calculated separately for the unfiltered data and for data filtered to show timescales shorter and longer than 10 yr, respectively.

Correlations are calculated between Tscan and each grid point in the selected SLP and North Atlantic SST fields. Correlations are also calculated between Tscan and three indices representative for the atmospheric circulation over the Scandinavian area. These indices are chosen to be similar to those used by Tuomenvirta et al. (2000) and Moberg et al. (2005), who studied relationships between Scandinavian temperatures and atmospheric circulation in observational data. These authors defined a zonal index (west–east wind flow), a meridional index (south–north wind flow) and an average pressure index (anticyclonic wind flow) by using SLP data from four stations. We choose SLP data from four grid points that correspond as closely as possible to the four stations. The four points are (clockwise, starting from the southernmost point): [15°E; 55°N], [5°E; 60°N], [15°E; 65°N], [25°E; 60°N]. The three indices are labelled SLPz (zonal), SLPm (meridional) and SLPa (average), where SLPz (SLPm) is the pressure difference between the southernmost and northernmost (easternmost and westernmost) grid points. SLPa is the average for the four grid points.

We perform also the correlation analysis between Tscan and SSTnor and Tnh. Correlations between Tscan and SSTnor reveal the strength of the relationship between Scandinavian temperatures and SSTs in an ocean region which is of importance for the Scandinavian climate. The correlations with Tnh have less obvious interpretations. Tnh may be thought of as an index containing information on the hemispheric integrated temperature response to external forcings (solar, volcanic and greenhouse gases), although it is also integrating all local and regional random temperature variations due to various circulation phenomena that are not related to the forcings. A strong correlation between Tscan and Tnh could thus indicate that Scandinavian

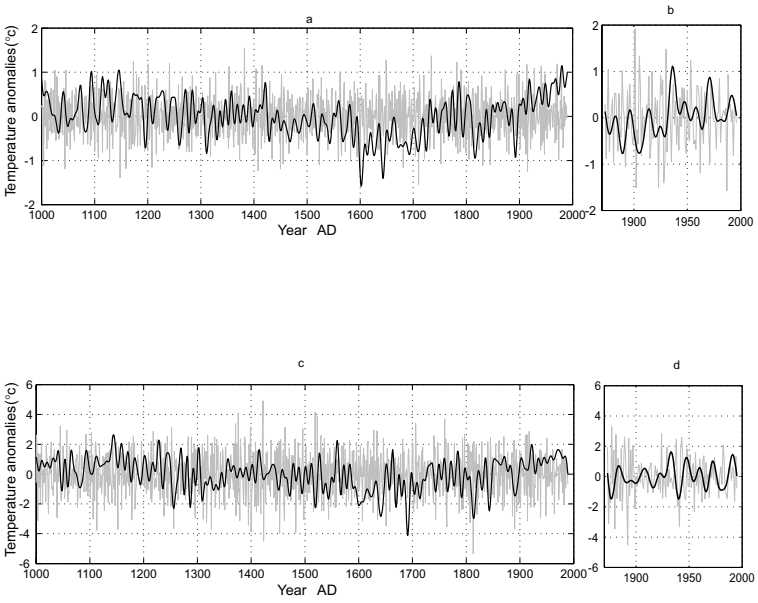

Fig. 2. Scandinavian temperatures from the simulation during 1000–1990 and observations during 1874–1996 in summer (JJA) (a–b) and winter (DJF) (c–d). Black lines show variability at timescales longer than 10 yr. Grey lines show shorter timescales. All data are shown as anomalies from the respective long-term means.

temperatures respond to the forcings in a similar manner as the entire NH. A strong correlation could also be expected if (forced or unforced) regional variability in the North Atlantic/North European sector (including Scandinavia) dominates the NH average temperatures. A weak correlation between Tscan and Tnh could indicate a strong role of area-restricted regional internal variability. It could, however, also be due to non-linear responses to the radiative forcings having a regional imprint that differs from the NH average response. An example is the observed and theorized effect from volcanic eruptions on the NAO, which lead to winter warming in Scandinavia but cooling in many other parts of the NH. Even if the interpretation of the Tscan/Tnh correlation is not straightforward, it may be argued that it can anyway be used for model evaluation. If the model behaves realistically, the same strength of correlation should be seen in the simulation as in the observations.

For the observational data, correlations between Tscan and the other variables are calculated over the 123 yr period 1874–1996. For the simulation, correlations are calculated for 10 century-long periods (1000–1099, 1100–1199, ..., 1800–1899, 1900–1990) and for the entire period 1000–1990. The correlation analysis for the 10 periods indicates how much the relationships can vary with time in the model, for periods of about the same length as the instrumental record. As regards low-frequency variability (>10 yr scales), the century long periods are very short and correlations are based on an effective number of degrees of freedom, that is, at most, only about 10. Therefore, low-frequency correlations can vary substantially between different periods. Similarly, the correlations obtained for the observational data are uncertain for the low-pass filtered data. The low-frequency correlation is much more reliable for the entire model simulation, which includes 991 yr of data.

The statistical significance of correlations is assessed with a Monte Carlo method suggested by Ebisuzaki (1997). With this method, a large number of time-series with the same spectral properties as the original ones are generated randomly. The significance level corresponds to the percentage of randomly generated correlations that are above (below) the observed positive (negative) correlations. For the SLP and SST fields, correlations are assessed by performing the significance test for each grid point. Significant correlations at the 0.1 level are shaded on the maps.

4.3. Response to volcanic forcing

To investigate the simulated temperature response in Scandinavia to the volcanic forcing, we use a compositing technique that is sometimes called superposed epoch analysis. The idea behind this method is to highlight the common response during the few years after selected large eruptions. Jones et al. (2003) discuss different variants of this technique, and references therein give examples of how the technique has been used. As suggested by Jones et al. (2003), we use high-pass filtered (>30 yr variability removed) and normalized monthly temperatures (their method 4). The response to the 10 strongest volcanic forcing events is studied. For each of the selected 10 eruption years, the 120 months of Tscan data centred on the January of the eruption year are extracted. Each month in each 120 month sequence is then expressed as a departure from the average of the appropriate pre-eruption months. The composite response is obtained from the average 10 yr sequence. The statistical significance of the composite response is determined using a Monte Carlo procedure, where the 0.05 significance level is determined from 20 000 randomly selected sets of ten 10 yr sequences in the Tscan series. This large number of realizations gives a robust test.

5. Results

5.1. Temporal evolution of multidecadal temperature variability

Figure 1d–e compares 30-yr-smoothed time-series for simulated Tscan and Tnh in summer (JJA) and winter (DJF), respectively. In both seasons the two series show a similar evolution, with warm conditions in the 12th century followed by a cooling trend to the 17th century and then a warming to the end of the simulation. This evolution is reminiscent of the concepts of a 'Medieval Warm Period' and a 'Little Ice Age' period deduced from analyses of various climate proxy data (see e.g. Brázdil et al., 2005; Matthews and Briffa, 2005; Osborn and Briffa, 2006). As the low-frequency evolution of the simulated Tscan so closely follows Tnh at these timescales, it seems that simulated Scandinavian low-frequency temperature variability largely responds to slow changes in radiative forcing in a manner similar to hemispheric temperatures. A part of the simulated cooling–warming secular trends over the millennium may also be due to a slow early adjustment of the model, from its supposed initial non-equilibrium with radiative forcing, in combination with the absence of anthropogenic aerosol forcing (see Section 2.3). Simulated temperatures in Scandinavia show a stronger variability compared to the NH (as expected because the Scandinavian region is much smaller), with notable multidecadal fluctuations between 1100–1300, 1600–1700 and 1800–1900. This suggests that regional processes related to circulation changes are important for the simulated Tscan variability.

5.2. Comparison with proxy data and long instrumental series

Figure 3a compares the evolution of the 30-yr-smoothed simulated April–August Tscan with the corresponding temperatures reconstructed for Northern Fennoscandia from tree rings and, after 1722, with instrumental temperatures for Uppsala. The simulated temperature evolution resembles rather well the reconstruction at multidecadal timescales from 1450 onward. Before this year there are clear discrepancies. The correlation

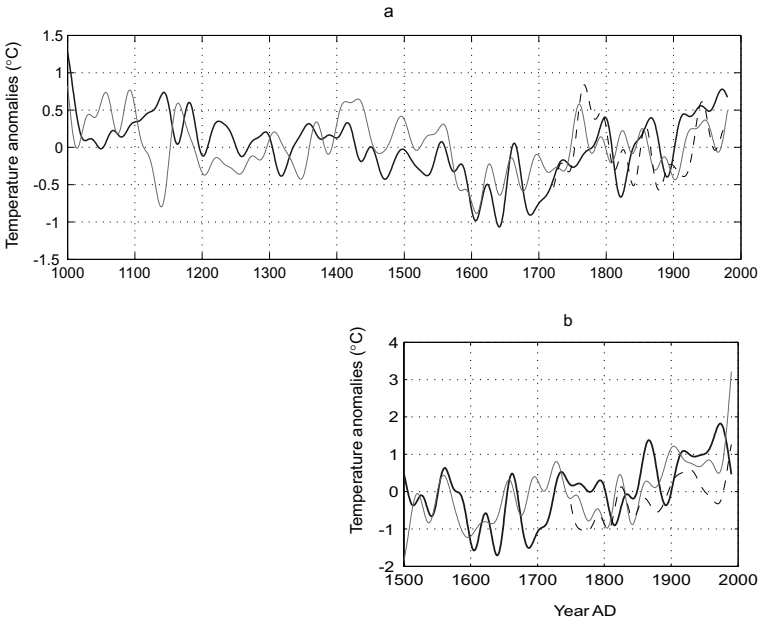

Fig. 3. Low-pass filtered (>30 yr scales) temperatures from the simulation (black), from reconstructions based on proxy data (grey) and instrumental data (dashed) for April–August (a) and December–March (b). The reconstruction in (a) is based on tree-ring width and densities from northern Fennoscandia. The reconstruction in (b) is a combination of documentary evidence for ice break-up dates and instrumental observations from Tallinn, Estonia. The instrumental data are from Uppsala, southern Sweden. All series are given as anomalies from their respective long-term means.

for smoothed data over the full period is 0.47, which is significant at the 0.05 level according to a Monte Carlo test. At higher frequencies the correlation is zero, as expected because the year-to-year variability is largely random variability. Comparison with Uppsala instrumental temperatures reveals some similarities in temporal evolution and amplitude of variations after the 1720s. There are, however, too cold simulated temperatures around 1700 (compared to tree-ring data) and during 1750–1780 (compared to Uppsala) and too high simulated temperatures in much of the 20th century (compared to both other series).

It should be noted that the three series represent different areas. However, this is not regarded as very serious as multidecadal variability should behave similarly within the rather small Scandinavian region. The poorer agreement between the tree-ring reconstruction and the simulation before around 1450 could be related to the fact that the reconstruction is based on fewer trees in its earlier part (Briffa et al., 1992), but it could also mean that the evolution of the simulated temperatures does not represent the real temperature evolution. The similarities after 1450 are nevertheless encouraging and the overall appearance in both the simulation and the tree-ring record, with a cooling trend from the 11th century to a minimum around 1600 followed by a warming, is in remarkable agreement.

The 30-yr-smoothed simulated December–March Tscan and the corresponding temperatures reconstructed for Tallinn based on ice-break up dates and instrumental data show an overall warming from around 1600 to the 20th century (Fig. 3b). The warming has similar magnitude in both series and the smoothed curves have about 40% common variance. Discrepancies appear mainly between 1690 and 1800 and near the beginning and end of the series. The latter discrepancies should not be overinterpreted, as low-pass filtered values are uncertain near the end points. The simulated temperatures from 1680 to 1730 are too cold compared to Tallinn data [and, by the way, too cold compared also to Scandinavian December–March temperatures in the reconstructions by Luterbacher et al. (2004) and Xoplaki et al. (2005); Jürg Luterbacher, personal communication, 2006]. Uppsala instrumental data after 1750 indicate that both the simulated Tscan and the observed Tallinn temperatures warm too much after the mid-19th century. The exaggerated recent warming in the Tallinn series could possibly be due to an insufficient correction of local urban warming.

Overall, the time evolution of the simulated Scandinavian winter temperatures appears to be rather realistic in winter during 1500–1990 as concerns low-frequency variability, although temporal details do not really match the empirical and instrumental evidence. This mismatch can reflect, for example, a dominance of internal regional temperature variability over the influence of external radiative forcings, or possibly be to an unrealistic response of simulated regional climate to the volcanic forcing, perhaps due to its crude representation in the model. The next section focusses on the simulated response to volcanic forcing.

5.3. Response to volcanic forcing

The simulated response of Tscan to the 10 strongest volcanic eruptions in the applied volcanic forcing history is analysed. These 10 events (Fig. 1b) occur in 1058, 1175, 1229, 1259, 1460, 1601, 1641, 1809, 1815 and 1831. Figure 4 shows, for each individual case and for the composite, the time sequence of normalized monthly temperature anomalies, starting with the January 5 yr before the eruption year (month –59) and ending with December in the fourth year after the eruption year (month 60). The January in the eruption year is assigned to month 1.

All monthly values are expressed as anomalies from the corresponding averages for the 5 pre-eruption years.

Individual eruptions show no clear response pattern if studied separately. In the composite, a clear organized response emerges with a cooling in the summer of the eruption year and in the three following summers. This response is significant at the 0.05 level. The magnitude of the simulated average cooling in summer is similar to that seen in instrumental temperature data from Scandinavia, after eight large tropical eruptions in the period since 1781 (Jones et al., 2003; their Fig. 4). In the instrumental record, however, a statistically significant summer cooling is seen only in year two and three after the eruptions. The absence of cooling in the first summer for the observational data is likely because some eruptions occurred too late in the year for an effect to be seen in the first summer, whereas in the model the volcanic forcing is always imposed from January. The agreement in the magnitude of the simulated and observed summer cooling is nevertheless remarkable, considering the crude parametrization of the volcanic forcing and the coarse horizontal resolution of the model.

In winter, we find no significant volcanic response of Scandinavian temperatures. In particular, we find no trace of the warming response that has been suggested from both theoretical and empirical viewpoints (Robock and Mao, 1992, 1995; Robock, 2000). Jones et al. (2003) found a warming of Scandinavian winter temperatures in the first, second and the fourth winter after large tropical eruptions (but a cooling in the third winter). However, the winter warming is not statistically significant in the observations (Jones et al., 2003). In the ECHO-G simulation of Scandinavian temperatures, only one single winter month nearly reaches the upper significance threshold in the composite, but this could be just a random occurrence. Several winter months in the few years after eruptions actually show insignificant negative deviations.

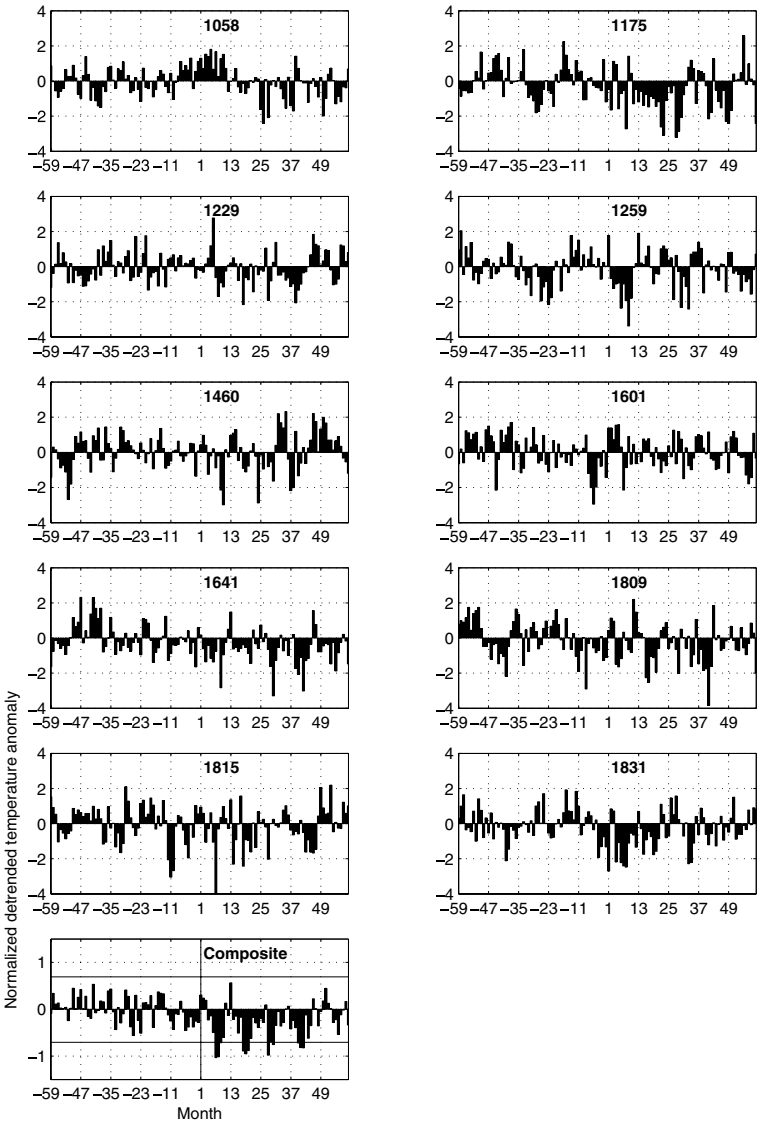

Fig. 4. Response of simulated Scandinavian temperatures to the 10 strongest volcanic forcing events. The response is shown for each individual event and for the composite average. Bars show standardized monthly temperature anomalies expressed as the deviation from the monthly anomalies in the 5 yr before the 'eruption year'. The time sequence goes from January 5 yr before the eruption year (month –59) to December 4 yr after the eruption year (month 60). Month 1 is January in the eruption year. The horizontal black lines in the composite show response thresholds at the 0.05 significance level.

In summary, the simulated average response of Tscan to large volcanic forcing events shows a similar cooling as seen in observations in the first few summers after the forcing events, but there is no trace of the observed warming response in winter. One may ask how these results are affected by the fact that, in some of the 10 cases, there occurs more than one strong negative forcing event within a 10 yr sequence. In particular, the event in 1809 (the fifth strongest forcing event) should influence temperatures in the 5 yr period before the event in 1815 (the third strongest). Therefore, we repeated the analysis with the 10 yr sequence centred on 1815 being replaced with the corresponding sequence for 1587 (the 11th strongest event). This change has a negligible effect on the results. To go one step further, we additionally replaced the sequence centred on 1460 (the nineth strongest event) with the sequence centred on 1453 (the 13th strongest). Also this replacement of data has negligible effects on the result. We conclude that the composite result in Fig. 4 is robust.

Yoshimori et al. (2005) used a similar representation of volcanic forcing in a simulation of the Maunder Minimum climate with the Community Climate System Model. They found a significant response of the NH atmospheric circulation towards an enhanced NAO pattern in the first two winters after volcanic forcing events. They also found an associated small winter warming in Scandinavia. This warming was, however, not significant at the 0.1 level, except for a small area that includes the southernmost tip of Scandinavia where significant warming was seen only in the second winter. Their result (winter warming in Scandinavia, but not significant) is thus in better agreement with results from instrumental data (Jones et al., 2003). The lack of a clear signal in our simulation may be due to a different response of our model to the same type of forcing. It is known that the NAO response to increases of greenhouse gas concentrations in simulations of the 21st century is strongly model dependent (Stephenson et al., 2006). It is therefore not unexpected to find model-related differences also in response to the crude effective volcanic forcing. Another possibility is that the response of the atmospheric circulation in our model may be geographically slightly shifted and does not directly affect the regional temperature index used here.

5.4. *Relationships between Scandinavian temperatures and atmospheric circulation, SSTs and NH temperatures*

Here, results are presented for instrumental and simulated data at both high and low frequencies (<10 yr and >10 yr variability) as well as for unfiltered data. To the extent practically possible, each partial result is first presented for observational data, followed by a comparison with simulated data. Then, the behaviour of the simulation is further reported and discussed.

5.4.1. Summer. Correlations, based on non-filtered observational data, between Tscan and the SLP field in summer (JJA) show a quadripolar pattern (Fig. 5a). One dipole is located over the Atlantic Ocean, with negative (positive) correlations north (south) of 50°N. The other dipole is located over Europe, with the largest positive correlations over northern Fennoscandia (+0.4) and negative correlations (−0.4) over the Black Sea. Correlations are significant at the 0.1 level over much of Fennoscandia and the eastern Mediterranean region. The strongest correlations in the western dipole are also significant. The western dipole (reminiscent of a positive NAO-phase) is considered to be less directly relevant for influencing Scandinavian temperatures, as it reflects an air flow pattern at a relatively long distance from Scandinavia. Previous results by, for example, Moberg et al. (2003; 2005) show

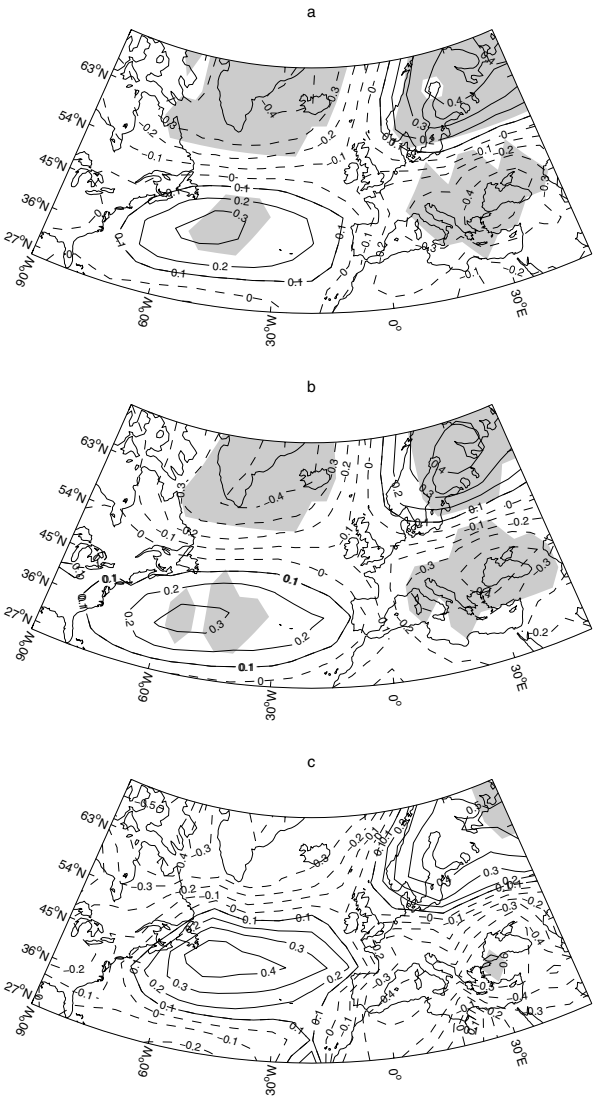

Fig. 5. Correlations in observational data between summer (JJA) temperatures in Scandinavia and SLPs over the North Atlantic and European sector. Correlations are calculated for 1874–1996 using unfiltered data (a), high-pass filtered data (timescales <10 yr) (b) and low-pass filtered data (timescales >10 yr) (c). Contour interval is 0.1. Shading indicates significance at the 0.1 level.

that warm summer temperatures over Scandinavia are associated with anticyclonic conditions, and conversely, cold temperatures with cyclonic conditions. The eastern dipole, in particular its northern part, is thus more directly relevant for this region. The correlations between Tscan and SLP are, however, rather weak ($r = 0.4$, i.e., only about 16% common variance).

Similar analyses are also made separately for high- and low-frequency observational data. In both cases, the correlations (Fig. 5b–c) are overall similar in both pattern and strength to those for unfiltered data (Fig. 5a). This suggests that, in reality, about the same rather weak relationship between summer temperature and atmospheric circulation occurs at high and low frequencies. At low frequencies, however, correlations are not significant due to fewer degrees of freedom. For simulated data, correlations between non-filtered Tscan and the SLP field is shown in Fig. 6 for each of the 10 centuries. Patterns with significant correlations similar to those in the observations occur in the eastern half of the domain, where an eastern dipole is seen in all 10 periods. A western dipole appears very weakly in only one of the 10 periods (1800–1899). Over Scandinavia, the maximum positive correlations vary between 0.1 and 0.5 among periods. Three of the periods have maximum correlations around 0.4 over northern Fennoscandia, that is, similar to the observations. We conclude that, over Scandinavia, the model quite well reproduces the observed relationships between temperatures and SLP in summer, but the relation with circulation over the western part of the study domain is not well reproduced.

Correlations calculated separately for high- and low-frequency data for the entire simulated period (maps not shown) indicate that the correlation pattern for the unfiltered simulated data (Fig. 6) is mainly associated with interannual variability, as the low-frequency correlation is close to zero all over the study

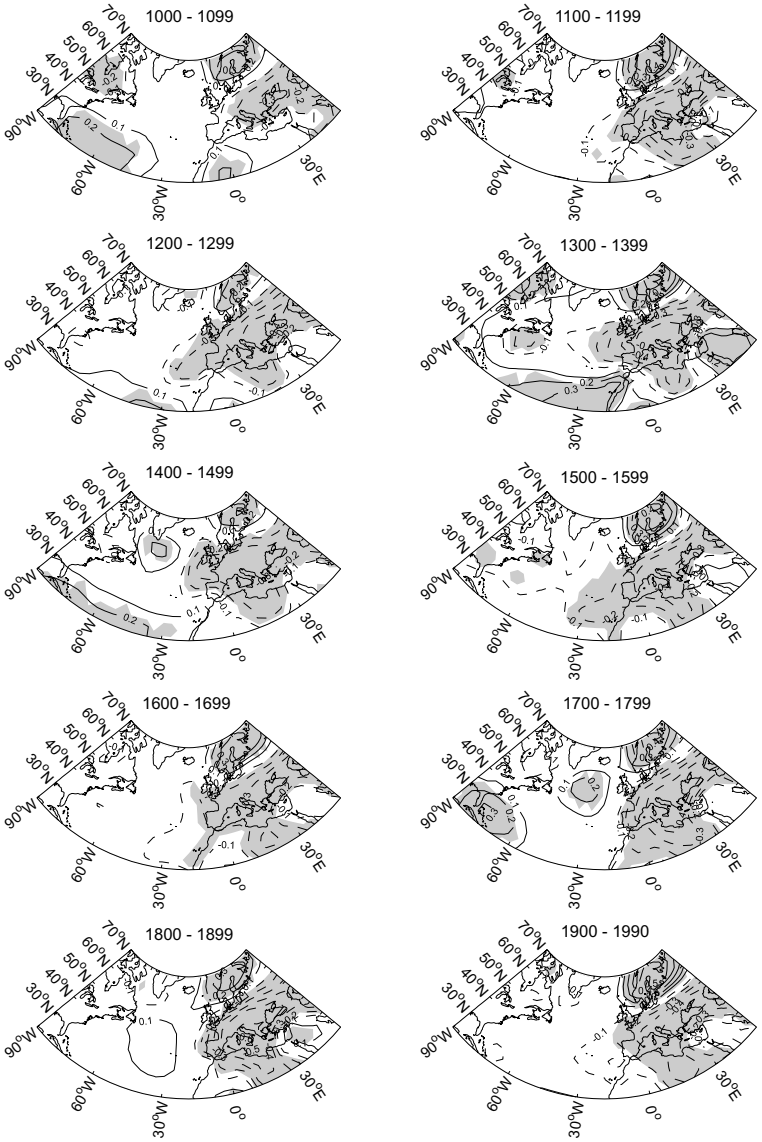

Fig. 6. Correlations in simulated data between summer (JJA) temperatures in Scandinavia and SLPs over the North Atlantic and European sector. Correlations are calculated for 10 century-long periods using unfiltered data. Contour interval is 0.1. Shading indicates significance at the 0.1 level.

Table 1. Correlations (×100) between Scandinavian summer (JJA) temperatures and five other indices. SLPz : zonal air flow, SLPm: meridional air flow, SLPa: average pressure, SSTnor: sea surface temperatures in the Norwegian Sea, Tnh: NH mean temperatures. Correlations are given for simulated and observational data at high and low frequencies (<10 yr and >10 yr timescales). For the simulation, correlations are given for the entire period 1000–1990 together with the minimum and maximum values among the 10 centuries. Correlations in observational data are calculated over 1874–1996. Asterisks denote significance at the 0.05 level.

	Simulated data							
	High frequency			Low frequency			Observed data	
Index (JJA)	1000–1990	Minimum	Maximum	1000–1990	Minimum	Maximum	High frequency	Low frequency
SLPz	−48*	−61*	−33*	−26*	−61*	0	−34*	−36*
SLPm	3	0	27*	7	−18	27	24*	22
SLPa	28*	9	41*	−6	−34*	36*	23	37*
SSTnor	47*	40*	53*	67*	32*	84*	76*	80*
Tnh	24*	15	34*	69*	26	71*	41*	57*

area. This suggests that there is no relationship between simulated summer Tscan and SLP at decadal and longer timescales, in opposite to the findings for observational data.

As regards correlations between observed Tscan and the North Atlantic SST field (maps not shown), we find that positive temperature anomalies in Scandinavia are associated with positive SST anomalies over the entire Atlantic Ocean. The strongest correlations (+0.6) occur over the Norwegian Sea. The corresponding simulated spatial pattern of correlations (also not shown) is quite similar to the observations, indicating a degree of realism in the simulation in this respect.

Table 1 gives the correlations between Tscan and the three circulation indices and SSTnor and Tnh for summer. At high frequency, correlations with the circulation indices are overall rather weak, but yet significant (at the 0.05 level) in some cases. In the observations, they are significant for SLPz (−0.34) and SLPm (+0.24). For SLPa the correlation is +0.23, but not significant.

In the model, high-frequency Tscan correlations with SLPz for the entire period (−0.48) is stronger than in the instrumental data. The SLPz correlation for the observations (−0.34) is near the 'weak' end of the range of corresponding century period values for the model (−0.33 to −0.61). For SLPm and SLPa, the ranges of simulated high-frequency correlations envelope the corresponding values from observational data, but in both cases the minimum correlations are very small and insignificant. For all three circulation indices, the difference between the maximum and minium correlations among century periods is about 0.3, indicating time-varying relationships.

High-frequency correlations between Tscan and SSTnor and Tnh are significant in the observational data (+0.76 and +0.41, respectively). The model data show significant correlations for these variables in the entire period, but they are weaker than in the observations and the maximum correlations among periods are weaker than for the observations in both cases. Nevertheless, even the minimum correlation between simulated Tscan and SSTnor is significant, indicating that there is always an association between these variables. For Tnh, however, the minimum correlation in the simulation is only +0.15 and not significant.

To summarize, for the high-frequency data, the model simulates quite realistic relationships between Tscan and the atmospheric circulation in summer. In the observations, Norwegian Sea SSTs show much stronger correlations than the circulation indices with Scandinavian temperatures, suggesting a major influence of the SST on the latter. The corresponding simulated relationship is too weak, but yet highly significant.

For the low-frequency observational data, we find about the same correlations as in the high-frequency data for all five indices. This suggests that, in the real world, the relationships are similar at high and low frequencies. This is not the case for the model data. In the entire simulation period, the associations with the circulation indices SLPz and SLPa are stronger for high frequencies than for low frequencies, whereas the correlations with SSTnor and Tnh are stronger for the low frequencies. These model results reveal that different factors influence the simulated Scandinavian summer temperatures at short and long timescales. At short timescales, variability in the atmospheric circulation is important although not determinant, whereas for long timescales this factor is rather unimportant. At long timescales, simulated summer Tscan is instead strongly correlated with SSTnor and Tnh. The strong low-frequency correlations with SSTnor and Tnh in the entire simulation period appear to be quite realistic, as they are rather similar to those for the observations. The range of low-frequency correlations among the 10 periods, however, is large due to the few degrees of freedom.

We conclude that the low-frequency evolution of simulated Scandinavian summer temperatures to a large extent follows the temperature evolution of the entire hemisphere (in agreement with the findings in Fig. 1d) and in the Norwegian Sea. This indicates that external forcing, or large-scale internal variability related to circulation processes in the North Atlantic Ocean, or a combination of these, are important factors for determining

simulated Scandinavian low-frequency temperature variability in summer. Atmospheric circulation processes appear to be less important.

5.4.2. Winter. In winter (DJF) correlations between unfiltered observed Tscan and the SLP field show a broad dipolar structure stretching over the North Atlantic and European area with negative (positive) values north (south) of about 52°–56°N (Fig. 7a). This is similar to the winter NAO pattern (Hurrell, 1995; Hurrell et al., 2003). Warm Scandinavian winters are thus related to a stronger than normal SLP gradient over the North Atlantic, bringing more maritime and mild air over much of Scandinavia. The correlations in winter are stronger (−0.6 over the northern Norwegian Sea and +0.5 over the Mediterranean) than in summer. Correlations at high and low frequencies (Fig. 7b–c) show very similar dipole patterns (but mostly insignificant at low-frequencies), suggesting an influence of the atmospheric circulation on temperature variability at both high and low frequencies in winter.

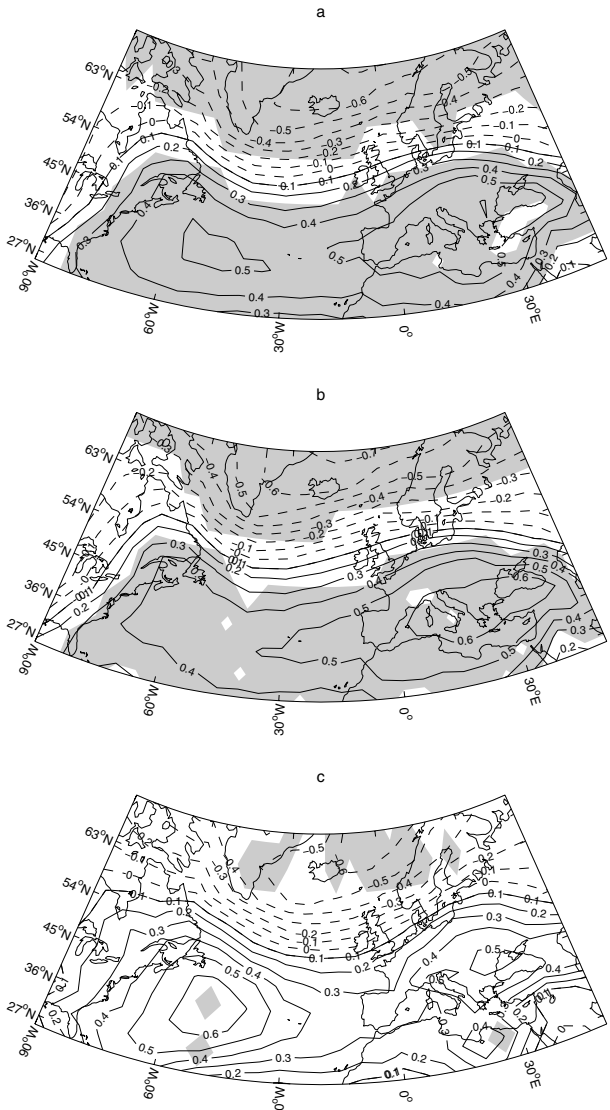

Fig. 7. As Fig. 5, but for winter (DJF).

In the simulation, the correlation patterns for all 10 periods (Fig. 8) are similar to the observed NAO-like pattern, with similar strengths and significant correlations. The ECHO-G model thus captures well the observed relationship between Scandinavian temperatures and SLP in winter. The main discrepancies between the 10 maps in Fig. 8 are seen south of 54°N. On some maps (1100–1199, 1200–1299, 1500–1599, 1600–1699) there are two regions with high positive correlations (one over the western Atlantic and one over the Mediterranean), whereas there is only one region with clear maximum correlations (in most cases over the Mediterranean) on the other maps. Such differences between periods are in broad agreement with changes in atmospheric regimes, as found by Casty et al. (2005a,b) in reconstructed 500 hPa pressure fields.

Correlations between the simulated Tscan and SLP field calculated separately for high and low frequencies (maps not shown) reveal patterns that are very similar to those for the unfiltered data. Thus the influence of the atmospheric circulation on simulated Scandinavian winter temperatures is almost the same for short and long timescales. This result clearly differs from the summer season, where the correlations are near zero for simulated low-frequency variability.

High-frequency correlations between Tscan and North Atlantic SSTs (not shown) are relatively weak in winter, except over the Norwegian Sea (+0.5) in both observed and simulated data. The relationships between Tscan and SSTs is much weaker in winter than in summer.

Correlations between winter Tscan and the other indices (SLPz, SLPm, SLPa, SSTnor and Tnh) are listed in Table 2. For high frequency, correlations in the observational data are significant for all indices except SLPm. It is particularly strong for SLPz (+0.74). For SLPa the correlation is much weaker and negative (−0.21), indicating only a weak association, where anticyclonic conditions correspond to cold Scandinavian winter temperatures.

In the simulation, high-frequency correlations for the entire period are rather similar to those in the observations, except for Tnh where the simulated relationship is near zero. This reveals that simulated high-frequency winter Tscan variations are decoupled from the Tnh variations in an unrealistic way (the correlation is +0.57 for observational data). Moreover, the simulated relation between Tscan and SSTnor appears to be slightly too weak. The simulated high-frequency relationships with the circulation indices show a range of 0.25–0.4 between the minimum and maximum correlations in the 10 centuries. Such variability in the relation between Scandinavian winter temperatures and circulation indices is in accord with unstable similar relationships seen in observational data (Chen and Hellström, 1999; Jacobeit et al., 2001; Slonosky et al., 2001), as well as with changes in the atmospheric regimes over Europe in winter (Casty et al., 2005a,b).

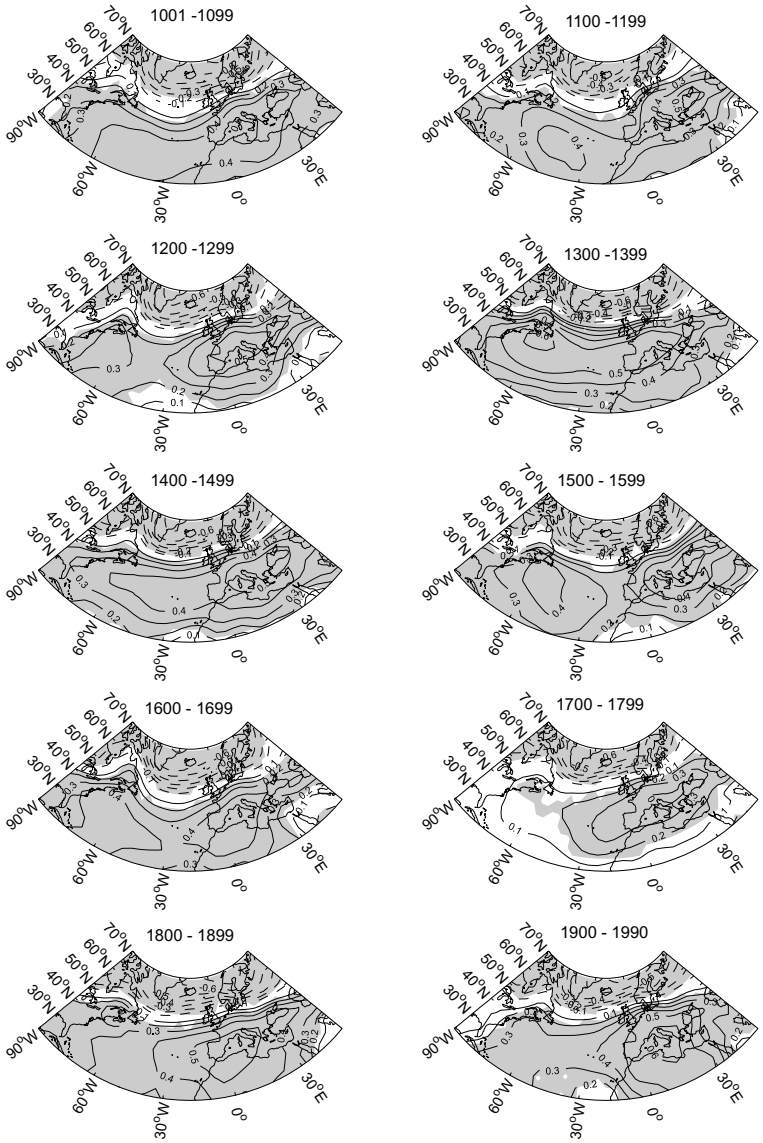

Fig. 8. As Fig. 6, but for winter (DJF).

The simulated low-frequency Tscan variability is significantly correlated with all five indices when the entire period is analysed. It is most strongly related to SLPz (+0.75), and somewhat weaker to Tnh (+0.62) and SSTnor (+0.55). The associations with SLPm and SLPa are much weaker. Low-frequency correlations with both SSTnor and Tnh are clearly stronger than their high-frequency counterparts. The observed low-frequency correlations lie within in the range enveloped by the 10 periods in the

Table 2. As Table 1, but for winter (DJF)

	Simulated data							
	High frequency			Low frequency			Observed data	
Index (DJF)	1000–1990	Minimum	Maximum	1000–1990	Minimum	Maximum	High frequency	Low frequency
SLPz	75*	64*	81*	75*	38*	90*	74*	68*
SLPm	−17	−31	0	−28*	−63*	36*	−8	34*
SLPa	−33*	−47*	−10	−26*	−65*	20	−21*	−23*
SSTnor	33	12	47*	55*	0	68*	43*	47*
Tnh	9	0	19	62*	20	75*	57*	18*

simulation for all indices except for Tnh. The ranges of simulated low-frequency correlations are, however, very large. Hence, with the exception of Tnh, it is nearly impossible to evaluate whether the simulated low-frequency relations are realistic by comparison with instrumental data. For Tnh it is tempting to conclude that the model overestimates the strength of the relationship, with a reservation for the uncertainty due to the shortness of the instrumental record.

For the three circulation indices, the low-frequency correlations in the entire simulation are quite similar to those at high frequencies, indicating that similar simulated circulation versus temperature relationships exist at high and low frequencies. This is supported by the fact that the simulated NAO index has a spectrum that is essentially white, when calculated for the entire simulation and for the 10-century-long independent periods. [The NAO spectrum is not shown, but Fig. 9b in the next section shows the simulated NAO pattern for December–March, defined as the leading Empirical Orthogonal Function (EOF) of the SLP field.] The simulated white noise spectrum for NAO is not in entire agreement with observations, as the observed NAO spectrum is slightly red (Hurrell et al., 2003).

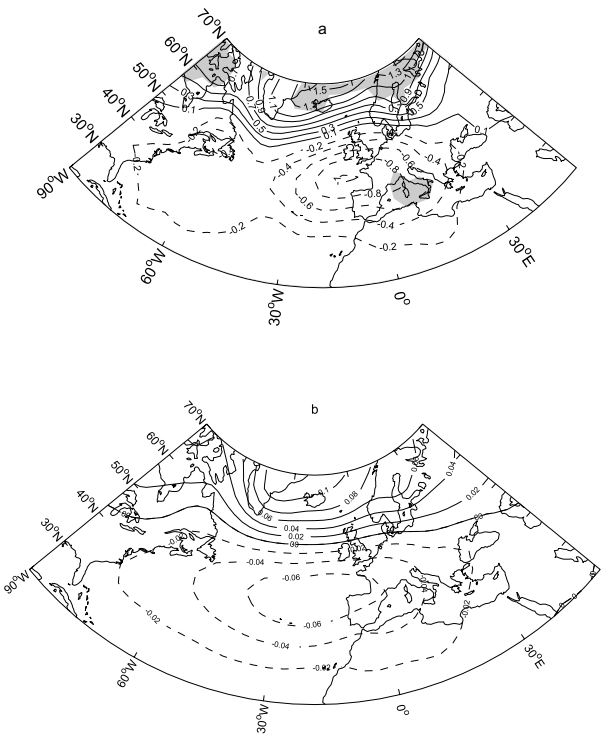

Fig. 9. Analysis of simulated SLPs for December–March over the North Atlantic and European sector. The map in (a) shows average anomalies for 1590–1650. Negative (positive) anomalies from the entire period 1000–1990 are represented by dashed (solid) lines. Contour interval is 0.2 hPa. Grey shading indicates significant anomalies at the 0.1 level. The map in (b) shows the leading EOF, which explains 37% variance, calculated for the period 1000–1990.

Overall, the relationships between Scandinavian winter temperatures and the atmospheric circulation pattern obtained for the ECHO-G model agree well with analyses of observational data (e.g. Hurrell, 1995; Chen and Hellström, 1999; Jacobeit et al., 2001; Marshall et al., 2001; Moberg et al., 2005). According to our correlation analysis, simulated Scandinavian winter temperatures are strongly related to the strength of the westerly wind flow at both high and low frequencies. A strong simulated association with SSTs in the Norwegian Sea and the NH mean temperatures, however, is seen only at low frequencies. The simulated low-frequency association with Tnh appears to be too strong, whereas the high-frequency associations with both Tnh and SSTnor are too weak.

6. Discussion

An evaluation of Scandinvian climate variability in a forced 1000 yrear simulation with ECHO-G has revealed both strong and weak points of the model. Observed relationships between Scandinavian temperature variations and atmospheric circulation patterns are overall well reproduced, particularly in winter. In summer, there appears to be too weak relationships between Scandinavian temperatures and large-scale atmospheric circulation patterns at longer than decadal timescales, but they are rather well simulated at shorter timescales.

The model exhibits some discrepancies from the observed covariations of Scandinavian temperatures with those of the entire NH and SSTs in the Norwegian Sea. In winter, at interdecadal timescales, simulated Scandinavian temperatures appears to covary too strongly with NH temperatures. Due to the shortness of the instrumental record, however, it is not really possible judge whether these simulated strong co-variations are unrealistic. In summer, at shorter timescales, the simulated co-variations with SSTs appears to be too weak. These properties have implications for the interpretation of both paleoclimate simulations and future climate scenarios derived from the model. For example, future scenarios of Scandinavian winter temperatures may possibly follow the NH temperature too strongly under the influence by slowly increasing greenhouse gas forcing, such that regional internal variations are suppressed. The model deficiencies found in our analysis also add further complexities to those discussed in Section 2.4, when comparison is made with proxy data. Deficiences like those observed here are likely common problems for many climate models (AchutaRao et al., 2004), but not unique to ECHO-G.

Bearing this in mind, some notable features of the simulated, and reconstructed, past Scandinavian temperatures are nevertheless worth a further discussion. The long-term evolution of the simulated Scandinavian temperatures, with cooling the the first half of the millennium and warming in the second half, goes much in parallel with the NH temperatures. Because these secular changes for the NH are certainly related to the long-term changes in external forcings, it is likely that much of the

simulated secular trends for Scandinavia have the same cause. The cooling in the early part is broadly in line with overall slowly decreasing solar forcing. However, a part of the early cooling can be explained by a slow adjustment of the model from an initial disequilibrium (Goosse et al., 2005; Osborn et al., 2006). The warming in the late part of the millennium can be explained by a combination of generally increasing solar forcing and, in particular after around 1850, the increasing greenhouse gas forcing. We note that warm-season northern Fennoscandian temperatures reconstructed from tree-ring data (Briffa et al., 1992) agree quite well with simulated temperatures in the last five centuries (Fig. 3a). Moreover, local proxy data for winter temperatures in the last five centuries (Tarand and Nordli, 2001) also agree with simulated temperatures (Fig. 3b). Due to these similarities, it is tempting to conclude that, in reality, a combination of external radiative forcings have determined much of the long-term evolution of past Scandinavian temperatures.

For the regional climate, it is of interest to understand the causes for the deviations from the long-term slow changes. The simulated Scandinavian temperatures (Fig. 1d–e) show a number of decadal and multidecadal warm and cold excursions from the long-term trends. We address some potential causes for some of the cold excursions.

The 30-yr-smoothed winter and summer temperatures (Fig. 1d–e) have prounced local minima around 1690, 1810–1820 and 1890. These correspond quite well with local minima in solar forcing, suggesting a trace of solar forcing influence on interdecadal temperature variations. However, the time point for the weakest solar forcing, around 1460, is not matched by any marked simulated temperature minimum. Furthermore, the absolute minimum of the simulated temperatures, near 1600, coincides with solar forcing being near its long-term average, it even shows a local maximum. Weakened solar forcing alone is thus not sufficient to explain pronounced regional cold intervals.

It has been noted previously, in studies of simpler climate models, (e.g. Bauer et al., 2003) that simulated large negative NH temperature anomalies occur when insolation minima coincide with large volcanic eruptions. Such models can, however, not take into account any complex dynamic response of the atmosphere to external forcings. As noted in the introduction, there is evidence from advanced models that volcanic eruptions can lead to a positive NAO phase (Yoshimori et al., 2005), while reduced solar forcing may trigger a negative NAO phase (Rind et al., 2004). Thus, these two effects may partly cancel each other in periods when volcanic eruptions coincide with solar minima. The resulting effect on Scandinavian temperatures would be difficult to predict. We note that, in our simulation, some local temperature minima coincide with periods of both volcanic eruptions and weak solar forcing—both for NH and Scandinavian temperatures. In particular, this happens for the simulated temperature minima around 1690 and 1810–1820. Hence, it appears that volcanic forcing can have contributed in this simulation with additional cooling to the weakened solar forcing—but this effect is only expected to take place in summer. Remember that the analysis of the simulated temperature response to volcanic forcing (Fig. 4) shows that only summer temperatures respond to this forcing. Furthermore, as discussed in Section 2.2 (e.g. Yoshimori et al., 2005), there is evidence that a warming of Scandinavian winters would be expected after large volcanic eruptions. Hence, cold winter spells in Scandinavia, both those simulated here and those in reality, are unlikely to be caused by volcanic forcing.

A candidate for causes of simulated cold spells in winter is internally generated circulation changes. The model evaluation revealed that simulated Scandinavian winter temperature variations are strongly associated, in a realistic way, with changes in zonal air flow both at short and long timescales. This factor could provide a potential explanation for cold intervals, as for example, the absolute minimum of the simulated Scandinavian winter temperatures. This minimum occurs just after 1600 in the 30-yr-smoothed series (Fig. 1e). The 10-yr-smoothed winter temperatures are systematically cold from around 1590 to 1650 (Fig. 2c). It is interesting to note that also winter temperatures reconstructed from proxy data (Fig. 3b) indicate cold conditions in reality in the same period. One may question whether the cold simulated—and real—Scandinavian winter temperatures during 1590–1650 could be due to an extended period with the NAO being largely in its negative phase, that is, with a weakened westerly wind flow towards Scandinavia?

In order to answer this question, we analyse the simulated mean December–March SLP field for the 1590–1650 period expressed as anomalies from its long-term mean. Figure 9a reveals a pattern that strongly resembles a negative NAO phase, with statistically significant weakenings of the Icelandic low and the Azores high pressure systems. These pressure anomalies indicate a weakening of the westerly flow to Scandinavia, leading to colder winter temperatures. In Fig. 9b we verify, by showing the leading EOF for the same data, that the pattern in Fig. 9a is indeed an NAO pattern. The first EOF explains 37% of the SLP variability, which is well in line with previous observational and model studies of the NAO (e.g. Luterbacher et al., 2002a; Hurrell et al., 2003; Min et al., 2005b). We conclude that the period 1590–1650 in the simulation is characterized by an average negative NAO phase, and that this can explain the simultaneous cold simulated winter conditions in Scandinavia.

It is noteworthy that also the winter NAO reconstruction by Luterbacher et al. (2002b) shows an average negative NAO phase during this period. However, this coincidence may be due to chance, since the relationship between the NAO phase and total external forcing in reality is not well established yet. Nevertheless, there is evidence for an important role of the atmospheric circulation on the Scandinavian cooling during 1590–1650 in both the simulation and the real world. A similar mechanism may also explain other cold intervals in winter. For example, Casty et al. (2005), based on an analysis of reconstructed 500 hPa fields (Luterbacher et al., 2002a), found a persistent occurrence

of blocking situations connected with colder temperatures in the period 1670–1700.

It is more difficult to explain the simulated cold summer temperatures that also occur in the period around 1590–1650 (Fig. 1d). We have not made any serious efforts to analyse the causes for this summer coldness. We note, however, that several large volcanic forcing events occur in this period (Fig. 1b). The temperature response to two of the strongest events, in 1601 and 1641, are shown in Fig. 4. A detailed inspection reveals that negative temperature anomalies in summer months occur up to 5 yr after both these eruptions. Inspection of the 10 yr low-pass filtered summer temperatures (Fig. 2a) shows that these two events are associated with strong cold summer temperature anomalies. Three less strong forcing events in the 1590–1650 period may have similar, but probably weaker, effects. The combined cooling effect from a sequence of five large volcanic forcing events during a few decades may thus have contributed to the simulated cold summer temperatures.

Another potential cause for cold simulated summers during 1590–1650 would be that the negative NAO phase in winter lead to colder winter SSTs over the north-eastern part of the North Atlantic Ocean and that this lead to cold temperatures in the following summers due to the large heat capacity of the ocean. We have not investigated this possible mechanism, but an analysis (not shown) of the lagged correlation between SSTs over the North Atlantic Ocean in observational data for May and Scandinavian temperatures in JJA reveals a relatively strong correlation (+0.5). This suggests that SSTs earlier in the year could modulate summer temperatures in Scandinavia. Moreover, as mentioned in the introduction, ocean dynamics can have an imprint on SST on longer timescales and therefore on the atmospheric circulation (e.g. Grötzner et al., 1998; Timmermann et al., 1998). Such mechanisms may have contributed to the cold simulated Scandinavian summer temperatures during 1590–1650. The fact that cold simulated summer temperatures in this period coincide with cold temperatures reconstructed from tree-ring data (Fig. 3a) encourages further studies in this respect.

Further model studies, combined with analyses of climate proxy data, can shed more light on the causes for past regional climate variations. Such studies should preferrably be made with ensembles of several simulations (Yoshimori et al., 2005). To achieve this, there is a need for more forced long AOGCM runs with different models—and also for more high-quality and high-resolution climate proxy data records.

7. Conclusions

The ECHO-G model, run with reconstructed solar, volcanic and greenhouse gas forcings for the last millennium, has been demonstrated to simulate quite realistically the observed relationships between atmospheric circulation and temperatures in Scandinavia for both summer and winter. Separate analyses of variability at timescales shorter and longer than 10 yr reveal that some, but not all, simulated relationships at the longer timescales are weaker than in instrumental observations in summer. In winter, the simulated relationships appear to be realistic at both short and long timescales.

Simulated relationships between Scandinavian summer temperature low-frequency variations and those of SSTs in the Norgwegian Sea and NH average temperatures are quite strong in both winter and summer. They are much weaker for high-frequency variations. Comparison with instrumental data reveal some unrealistic model behaviour, with a tendency of too weak high-frequency co-variations. Low-frequency co-variations with NH winter temperatures appear to be too strong.

The simulated Scandinavian temperatures show a realistic cooling response to volcanic forcing in the first few summers after strong forcing events, but there is no trace of the warming response in winter that has been found in observational data and other modelling studies. The lack of winter warming response in ECHO-G could be related to the crude representation of the volcanic forcing, which is imposed only as a change in effective solar radiation.

The time evolution of simulated Scandinavian April–August temperatures broadly follows the corresponding temperatures reconstructed from tree-ring data in northern Fennoscandia. This includes a cooling in the first half of the millennium and a warming in the second half. The overall temperature evolution in winter is similar, but comparison with winter temperature proxy data can only be made for the last 500 yr, when proxy data are in agreement concerning an overall warming trend. The secular cooling–warming behaviour can largely be explained by slow changes radiative forcings, but the amplitude is likely somewhat too large due to too cold initial temperatures and the omission of anthropogenic aerosol forcing in the simulation.

Decadal and multidecadal deviations from the centennial cooling–warming pattern seem to be the result of a mixture of causes. Temporary decreases in solar radiation can explain some cold intervals in both winter and summer. Sequences with strong volcanic forcing events can also contribute in summer. The coldest period in the simulation occurs between 1590 and 1650 in both winter and summer. In winter this cold period is associated with an average negative NAO phase in the simulation. This can explain the systematically low winter temperatures, through a weakened westerly flow of mild air. It is more difficult to explain why simulated summer temperatures are also at their minimum in the same period. Several strong volcanic forcing events between 1590 and 1650 seem to have contributed to the cold summers. We also speculate that cold summer temperatures in this period can be connected to the NAO-related winter coldness, which, in combination with the large heat capacity of the neighbouring ocean, could help keep the Scandinavian summer temperatures rather low. It is noteworthy that cold conditions in this period are also recorded in Scandinavian proxy data for both

winter and summer and, moreover, that other proxy data suggest an average negative NAO phase in winters in the same period.

Acknowledgments

The study was made as part of the project 'A 2000-year climate reconstruction for Sweden', funded by the Swedish Nuclear Fuel and Waste Management Co. (Grant to AM and Barbara Wohlfarth, same department as IG). AM was also funded by the Swedish Research Council. The work by EZ is part of the EU Project SOAP. Phil Jones provided the tree-ring series and Øyvind Nordli the ice break-up series. We thank two anonymous reviewers, in particular Reviewer 2, for clear and constructive suggestions for how to revise earlier versions of this paper.

References

AchutaRao, K., Covey, C., Doutriaux, C., Fiorino, M., Gleckler, P. and co-authors. 2004. An appraisal of coupled climate model simulations. UCRL-TR-200550, Lawrence Livermore National Laboratory, California, 183 pp.

Bard, E., Raisbeck, G. Yiou, F. and Jouzel, J. 2000. Solar irradiance during the last 1200 years based on cosmogenic nuclides. *Tellus* **52B**, 985–992.

Basnett, T. and Parker, D. 1997. Development of the Global Mean Sea Level Pressure Data Set GMSLP2. Climate Research Technical note, 79, Hadley Centre, Meteorological Office, Exeter, UK.

Bauer, E., Claussen, M., Brovkin, V. and Huenerbein, A. 2003. Assessing climate forcings of the Earth system for the past millennium. *Geophys. Res. Lett.* **30**(6), 1276, doi:10.1029/2002GL016639.

Bellouin, N., Boucher, O. Haywood, J. and Reddy, M. S. 2005. Global estimate of aerosol radiative forcing from satellite measurements. *Nature* **438**, 1138–1141.

Bergström, H. and Moberg, A. 2002. Daily air temperature and pressure series for Uppsala (1722–1998). *Climatic Change* **53**, 213–252.

Bertrand, C., Loutre, M.-F., Crucifix, M. and Berger, A. 2002. Climate of the last millennium: a sensitivity study. *Tellus* **54A**, 221–244.

Bjerknes, J. 1962. Synoptic survey of the interaction of sea and atmosphere in the North Atlantic. Geofysiske Publikasjoner, *Geophysica Norvegica* **24**, 115–145.

Brázdil, R., Pfister, C., Wanner, H., von Storch, H. and Luterbacher, J. 2005. Historical climatology in Europe—the state of the art. *Climatic Change* **70**, 363–430.

Briffa, K. R., Jones, P. D., Bartholin, T. S., Eckstein, D., Schweingruber, F. H. and co-authors. 1992. Fennoscandian summers from AD 500: temperature changes on short and long time scale. *Climate Dyn.* **7**, 111–119.

Bürger, G., Fast, I. and Cubasch, U. 2006. Climate reconstruction by regression—32 variations on a theme. *Tellus* **58A**, 227–235.

Casty, C., Handorf, D., Raible, C. C., González-Rouco, J. F., Weisheimer, A., Xoplaki, E. and co-authors. 2005a. Recurrent climate winter regimes in reconstructed and modelled 500 hPa geopotential height fields over the North Atlantic/European sector 1659–1990. *Climate Dyn.* **24**, 809–822.

Casty, C., Handorf, D. and Sempf, M. 2005b. Combined winter climate regimes over the North Atlantic/European sector 1766–2000. *Geophys. Res. Lett.* **32**, L13801, doi:10.1029/2005GL022431.

Chen, D. 2000. A monthly circulation climatology for Sweden and its application to a winter temperature case study. *Int. J. Climatol.* **20**, 1067–1076.

Chen, D. and Hellström, C. 1999. The influence of the North Atlantic Oscillation on the regional temperature variability in Sweden: spatial and temporal variations. *Tellus* **51A**, 505–516.

Crowley, T. 2000. Causes of climate change over the past 1000 years. *Science* **289**, 270–276.

Ebisuzaki, W. 1997. A method to estimate the statistical significance of a correlation when the data are serially correlated. *J. Climate* **10**, 2147–2153.

Etheridge, D. M., Steele, L. P., Langenfelds, R. L., Francey, R. J., Barnola, J.-M. and co-authors. 1996. Natural and anthropogenic changes in atmospheric CO_2 over the last 1000 years from air in Antarctic ice and firn. *J. Geophys. Res.* **101** (D2), 4115–4128.

Etheridge, D. M., Steele, L. P., Francey, R. J. and Langenfelds, R. L. 1998. Atmospheric methane between 1000 A.D. and present: Evidence of anthropogenic emissions and climatic variability. *J. Geophys. Res.* **103**(D13), 15979–15994.

Fisher-Bruns, I., von Storch, H., González-Rouco, J. F. and Zorita, E. 2005. Modelling the variability of midlatitude storm activity on decadal to century time scales. *Climate Dyn.* **25**, 461–476.

Foukal, P., North, G. and Wigley, T. 2004. A stellar view on solar variations and climate. *Science* **306**, 68–69.

Goosse, H., Renssen, H., Timmermann, A. and Bradley, R. 2005. Internal and forced climate variability during the last millennium: a model-data comparison using ensemble simulations. *Quat. Sci. Rev.* **24**, 1345–1360.

González-Rouco, J. F., von Storch, H. and Zorita, E. 2003. Deep soil temperature as proxy for surface air-temperature in a coupled model simulation of the last thousand years. *Geophys. Res. Lett.* **30**(21), 2116, doi:10.1029/2003GL018264.

González-Rouco, J. F., Beltrami, H., Zorita, E. and von Storch, H. 2006. Simulation and inversion of borehole temperature profiles in surrogate climates: Spatial distribution and surface coupling. *Geophys. Res. Lett.* **33**, L01703, doi:10.1029/2005GL024693.

Grötzner, A., Latif, M. and Barnett, T. P. 1998. A decadal climate cycle in the North Atlantic Ocean as simulated by the ECHO coupled GCM. *J. Climate* **11**, 831–847.

Hurrell, J. W. 1995. Decadal trends in the North Atlantic Oscillation: regional temperatures and precipitation. *Science* **269**, 676–679.

Hurrell, J. W., Kushnir, Y., Ottersen, G. and Visbeck, M. 2003. An overview of the North Atlantic Oscillation. In: *The North Atlantic Oscillation. Climatic Significance and Environmental Impact* (eds.J. W. Hurrell, Y. Kushnir, G. Ottersen and M. Visbeck). Geophysical Monograph 134, American Geophysical Union, Washington, D.C., pp. 1–35.

IPCC. 2001. Climate change 2001: The scientific basis. In: *Contribution of Working group I to the Third Assessment Report of the Intergovermental Panel of Climate Change* (eds.J. T. Houghton, Y. Ding, D. J. Griggs, M. Noguer, P. J. van der Linden and co-editors). Cambridge University Press, Cambridge, UK and New York, USA, 881 pp.

Jacobeit, J., Jönsson, P., Bärring, L., Beck, C. and Ekström, M. 2001. Zonal indices for Europe 1780–1995 and running correlations with temperature. *Climatic Change* **48**, 219–241.

Jones, G. S., Gregory, J. M., Stott, P. A., Tett, S. F. B. and Thorpe, R. B. 2005. An AOGCM simulation of the climate response to a volcanic super-eruption. *Climate Dynamics* **25**, 725–738.

Jones, P. D. and Moberg, A. 2003. Hemispheric large-scale surface air temperature variations: an extensive revision and an update to 2001. *J. Climate* **16**, 206–223.

Jones, P. D., Moberg, A., Osborn, T. J. and Briffa, K. R. 2003. Surface climate responses to explosive volcanic eruptions seen in long European temperature records and mid-to-high latitude tree-ring density around the Northern Hemisphere. In: *Volcanism and the Earth's Atmosphere* (eds.A. Robock and C. Oppenheimer). Geophysical Monograph 139. American Geophysical Union, Washington, D.C., pp. 239–254.

Kaplan, A., Cane, M., Kushnir, Y., Clement, A., Blumenthal, M. and co-authors 1998. Analyses of global sea surface temperature 1856–1991. *J. Geophys. Res.* **103**, 18567–18589.

Kodera, K. 1994. Influence of volcanic eruptions on the troposphere through stratospheric dynamical processes in the Northern Hemisphere winter. *J. Geophys. Res.* **99**(D1), 1273–1282.

Lean, J. and Rind, D. 2001. Earth's response to a variable sun. *Science* **292**, 234–236.

Lean, J., Beer, J. and Bradley, R. 1995. Reconstruction of solar irradiance since 1610: Implications for climate change. *Geophys. Res. Lett.* **22**, 3195–3198.

Lean, J. L., Wang, Y.-M. and Sheeley, Jr., N. R. 2002. The effect of increasing solar activity on the Sun's total and open magnetic flux during multiple cycles: Implications for solar forcing of climate. *Geophys. Res. Lett.* **29**, 2224, doi:10.1029/2002GL015880.

Legutke, S. and Voss, R. 1999. The Hamburg Atmosphere-Ocean coupled circulation model ECHO-G. Technical Report 18, DKRZ, Hamburg, 62 pp.

Luterbacher, J., Xoplaki, E., Dietrich, D., Rickli, R., Jacobeit, J. and co-authors. 2002a. Reconstruction of sea level pressure fields over the Eastern North Atlantic and Europe back to 1500. *Climate Dyn.* **18**, 545–561.

Luterbacher, J., Xoplaki, E., Dietrich, D., Jones, P. D., Davies, T. D. and co-authors. 2002b. Extending North Atlantic Oscillation reconstructions back to 1500. *Atmos. Sci. Lett.* **20**, doi:10.1006/asle.2001.0044.

Luterbacher, J., Dietrich, D., Xoplaki, E., Grosjean, M. and Wanner, H. 2004. European seasonal and annual temperature variability, trends and extremes since 1500. *Science* **303**, 1499–1503.

Marshall, J., Kushnir, Y., Battisti, D., Chang, P., Czaja, A. and co-authors. 2001. North Atlantic climate variability: phenomena, impacts and mechanisms. *Int. J. Climatol.* **21**, 1863–1898.

Matthews, J. A. and Briffa, K. R. 2005. The 'Little Ice Age': Re-evaluation of an evolving concept. *Geogr. Ann.* **87A**, 17–36.

Min, S.-K., Legutke, S., Hense, A. and Kwon, W.-T. 2005a. Internal variability in a 1000-yr control simulation with the coupled climate model ECHO-G—I. Near-surface temperature, precipitation and mean sea levelpressure. *Tellus* **57A**, 605–621.

Min, S.-K., Legutke, S., Hense, A. and Kwon, W.-T. 2005b. Internal variability in a 1000-yr control simulation with the coupled climate model ECHO-G-II. El Niño Southern Oscillation and North Atlantic Oscillation. *Tellus* **57A**, 622–640.

Moberg, A., Alexandersson, H., Bergström, H. and Jones, P. D. 2003. Were southern Swedish summer temperatures before 1860 as warm as measured? *Int. J. Climatol.* **23**, 1495–1521.

Moberg, A., Tuomenvirta, H. and Nordli, Ø. 2005. Recent climatic trends. In: *The Physical Geography of Fennoscandia. Oxford Regional Environments Series* (ed.M Seppälä) Oxford University Press, Oxford, 113–133.

Osborn, T. J. and Briffa, K. R. 2006. The spatial extent of 20th-century warmth in the context of the past 1200 years. *Science* **311**, 841–844.

Osborn, T.J. , Raper, S. C. B. and Briffa, K. R. 2006. Simulated climate change during the last 1000 years: comparing the ECHO-G general circulation model with the MAGICC simple climate model. *Climate Dyn.* **27**, 185–197.

Pauling, A., Luterbacher, J., Casty, C. and Wanner, H. 2006. Five hundred years of gridded high-resolution precipitation reconstructions over Europe and the connection to large-scale circulation. *Climate Dyn.* **26**, 387–405.

Raible, C. C., Luksch, U., Fraedrich, K. and Voss, R. 2001. North Atlantic decadal regimes in a coupled GCM simulation. *Climate Dyn.* **18**, 321–330.

Raible, C. C., Stocker, T. F., Yoshimori, M., Renold, M. and Beyerle, U. 2005. Northern hemispheric trends of pressure indices and atmospheric circulation patterns in observations, reconstructions, and coupled GCM simulations. *J. Climate* **18**, 3968–3982.

Raymond, W. and Garder, A. 1991. A review of recursive and implicit filters. *Mon. Wea. Rev.* **119**, 477–495.

Reid, G. C. 1991. Solar total irradiance variations and the global sea surface temperature record. *J. Geophys. Res.* **96** (D2), 2835–2844.

Rind, D., Shindell, D., Perlwitz, J. and Lerner, J. 2004. The relative importance of solar and anthropogenic forcing of climate change between the Maunder Minimum and the present. *J. Climate* **17**, 906–929.

Robertson, A., Overpeck, J., Rind, D., Mosley-Thompson, E., Zielinski, G. and co-authors. 2001. Hypothesized climate forcing time series for the last 500 years. *J. Geophys. Res.* **106**(D14), 14783–14803.

Robock, A. 2000. Volcanic eruptions and climate. *Rev. Geophys.* **38**, 191–219.

Robock, A. 2002. The climatic aftermath. *Science* **295**, 1242–1244.

Robock, A. and Mao, J. 1992. Winter warming from large volcanic eruptions. *Geophys. Res. Lett.* **12**, 2405–2408.

Robock, A. and Mao, J. 1995. The volcanic signal in surface temperature observations. *J. Climate* **8**, 1086–1103.

Roeckner, E., Arpe, K., Bengtsson, L., Christoph, M., Clausen, M. and co-authors. The atmospheric general circulation model ECHAM4: Model description and simulation of present-day climate. MPI Report No. 218, Max-Planck-Institut für Meteorologie, Hamburg, Germany, 90 pp.

Siegenthaler, U., Monnin, E., Kawamura, K., Spahni, R., Schwander, J. and co-authors. 2005. Supporting evidence from the EPICA Dronning Maud Land ice core for atmospheric CO_2 changes during the past millennnium. *Tellus* **57B**, 51–57.

Slonosky, V. C., Jones, P. D. and Davies, T. D. 2001. Atmospheric circulation and surface temperature in Europe from the 18th century to 1995. *Int. J. Climatol.* **21**, 63–75.

Stendel, M., Mogensen, I. A. and Christensen, J. H. 2006. Influence of various forcings on global climate in historical times using a coupled atmosphere-ocean general circulation model. *Climate Dyn.* **26**, 1–15.

Stephenson, D. B., Pavan, V., Collin, M., Junge, M. M., Quadrelli, R. and Participating CMIP2 Modelling Groups. 2006. North Atlantic Oscillation response to transient greenhouse gas forcing and the impact in European winter climate: a CMIP2 multi-model assessment. *Climate Dyn.* **27**, 401–420.

Tarand, A. and Nordli, P. Ø. 2001. The Tallinn temperature series reconstructed back half a millennium by use of proxy data. *Climatic Change* **48**, 189–199.

Taylor, K. E. and Penner, J. E. 1994. Response of the climate system to atmospheric aerosols and greenhouse gases. *Nature* **369**, 734–737.

Tett, S. F. B., Betts, R., Crowley, T. J., Gregory, J., Johns, T. C. and co-authors. 2006. The impact of natural and anthropogenic forcings on climate hydrology since 1550. *Climate Dyn.*, published online, doi: 10.1007/s00382-006-0165-1.

Timmermann, A., Latif, M., Voss, R. and Grötzner, A. 1998. Northern interdecadal variability: A coupled air-sea mode. *J. Climate* **11**, 1906–1931.

Tuomenvirta, H., Drebs, A., Frich, P. and Nordli, P. Ø. 2000. Trends in Nordic and Arctic temperature extremes and ranges. *J. Climate* **13**, 977–990.

Visbeck, M., Chassignet, E. P., Curry, R. G., Delworth, T. L., Dickson, R. R. and co-authors. 2003. The ocean's response to North Atlantic Oscillation variability. In: *The North Atlantic Oscillation. Climatic Significance and Environmental Impact* (eds.J. W. Hurrell, Y. Kushnir, G. Ottersen and M. Visbeck). Geophysical Monograph 134, American Geophysical Union, Washington, D.C., pp. 113–145.

von Storch, H., Zorita, E., Jones, J. M., Dimitriev, Y., González-Rouco, F. and co-authors. 2004. Reconstructing past climate from noisy data. *Science* **306**, 679–682.

von Storch, H., Zorita, E., Jones, J. M., Dimitriev, Y., González-Rouco, F. and co-authors. 2006. Response to comment on "Reconstructing Past Climate from Noisy Data". *Science* **312**, doi:10.1126/science.

Walker, G. T. and Bliss, E. W. 1932. World Weather V. *Mem. Roy. Met. Soc.* **4**, 53–84.

Wolff, J.-O., Maier-Reimer, E. and Legutke, S. 1997. The Hamburg Ocean Primitive Equation Model. Technical report No. 13, German Climate Computer Center (DKRZ), Hamburg, 98 pp.

Xoplaki, E., Luterbacher, J., Paeth, H., Dietrich, D., Steiner, N., Grosjean, M. and Wanner, H. 2005. European spring and autumn temperature variability and change of extremes over the last half milliennium. *Geophys. Res. Lett.* **32**, L15713, doi: 10.1029/2005GL023424.

Yoshimori, M., Stocker, T. F., Raible, C. C. and Renold, M. 2005. Externally forced and internal variability in ensemble climate simulations of the Maunder Minimum. *J. Climate* **18**, 4253–4270.

Zorita, E., von Storch, H., Gonzalez-Rouco, F. J., Cubash, U., Luterbacher, J. and co-authors. 2004. Climate evolution in the last five centuries simulated by an atmosphere-ocean model: global temperatures, the North Atlantic Oscillation and the Late Maunder Minimum. *Meteorologische Zeitschrift* **13**, 271–289.